New Insights on the Interstellar Medium from EUV Observations

STUART BOWYER

Center for EUV Astrophysics, 2150 Kittredge Street,
University of California, Berkeley, CA 94720–5030, USA

Observations in the EUV band have provided new insights into the interstellar medium. In the following I discuss two areas in which EUV observations are providing unique information: the ionization state of the ISM, and the pressure of the hot phase of the local interstellar medium and the bearing of this work on the McKee-Ostriker model of the ISM.

1. The Pressure of the Hot Phase of the Local Interstellar Medium and Implications Regarding the Mckee-Ostriker Model

Numerous estimates of the state of the hot ISM have been made based on theoretical models and meager observational data. In Table 1, I list some of the estimates of this pressure. They are highly disparate.

In principle, the pressure can be obtained directly from the relation:

$$P = 1.92kT\sqrt{EM/L} \tag{1.1}$$

where T is the temperature, EM is the emission measure, L is the line-of-sight length of the emitting region, k is Boltzmann's constant and the factor of 1.92 is appropriate for the total number of particles in a near fully-ionized plasma that is 90% hydrogen and 10% helium.

A number of shadows have been detected in the X-ray background; I summarize these in Table 2. I also list an EUV shadow detected with *EUVE*. Attempts have been made to use shadows in the X-ray background to obtain the pressure of the hot phase of the ISM using Equation 1.1. Unfortunately, because of the relatively high transmission of the ISM to X-rays, the X-ray flux observed is a mixture of nearby emission convolved with partially absorbed emission from more distant regions. Nonetheless, estimates of the pressure have been made from the X-ray measurements using various assumptions and extensive modeling; I list the result of one recent analysis using X-ray shadows in Table 1. In Table 2 I also list the wavelengths of the bandpasses of the X-ray observations of cloud shadows at 10% of peak transmission. I also show the mean effective wavelength determined by a weighted integral over a nominal plasma spectrum having $T = 7 \times 10^5$ K and a foreground H I column of $N_{\rm H} = 5 \times 10^{18}$ cm^{-2} to account for absorption by the local cloud around the sun. Finally, I show the column density of hydrogen associated with a non-depleted ISM that would produce one optical depth of absorption for the mean effective wavelength of the observation. The substantial column needed to absorb X-rays highlights the difficulties of using cloud shadows in the X-ray band to define a definitive emission path length.

During the Extreme Ultraviolet Explorer's all-sky survey, a long exposure along the ecliptic plane was obtained by the deep survey telescope. Only part of this data has been fully analyzed but in the analyzed data an EUV shadow was detected in the Lexan/boron (Lx/B) filter (65–190 Å) (Lieu et al. 1993). A statistical analysis using a sliding rectangular box of 0.3° width revealed that the core of this shadow is 3.9 σ below the average background. I show the relevant parameters of this observation in Table 2.

In contrast with X-ray shadow data, EUV shadows have great potential for determining

S. Bowyer and R. F. Malina (eds.), Astrophysics in the Extreme Ultraviolet, 255–260.

TABLE 1. Estimates of the Hot ISM Pressure

Method	Reference	P/k, K/cm^3
Static snr model	Cox & Reynolds 1987	10000
Halo equilibrium model	Spitzer 1990	11000 (thermal plus magnetic)
C IV & O III] emission data	Martin & Bowyer 1990 (corrected)	3000
CIV modeled to midplane	Shull & Slavin 1994	4400–7400
Pressure equilibrium with cool diffuse clouds	Data from Jenkins, Jura & Loewenstein 1983	280–50,000 4000 (typical)
X-ray shadows	Snowden, McCammon, & Verter 1993	12500

TABLE 2. Shadows in the Diffuse Background

Instrument	Reference	Band (keV)	10% Wavelengths (Å)	Mean Wavelength (Å)	$N_{H\,I}$ at $1/e$ (cm^{-2})
ROSAT PSPC	Burrows & Mendenhall 1991; Snowden et al. 1991	0.25	44–85	69	1×10^{20}
	Snowden, McCammon, & Verter 1993	0.75	11–25	18	2×10^{21}
	Snowden, McCammon, & Verter 1993	1.5	7–10	8	1×10^{22}
EUVE DS	Bowyer et al. 1995	Lx/B	65–190	116	2×10^{19}

the pressure of the local ISM because EUV emission is completely absorbed by even thin clouds, thus defining the path length of the region observed. Bowyer et al. (1995) have compared the EUV cloud shadow data with *IRAS* 100 μm flux averaged over the deep survey telescope field of view. In the *IRAS* data, compact molecular clouds and isolated cirrus appear as enhanced features above the background levels established by zodiacal light and diffuse cirrus. This background was fitted by a cubic spline function and was subtracted to isolate discrete clouds. An enhancement was found in the *IRAS* data which is aligned with the EUV absorption dip.

The mean intensity of the *IRAS* feature averaged over the 3 σ EUV absorption region is 0.518 MJy sr^{-1} above the baseline *IRAS* flux. Using a standard conversion ratio, the associated hydrogen column is 6×10^{19} cm^{-2}. This is about three optical depths at the mean wavelength of the *EUVE* Lx/B filter. Hence EUV flux from behind the cloud is completely attenuated, and the count rate in the direction of the cloud in this band is due entirely to foreground emission.

Bowyer et al. determined the distance to the EUV-absorbing cloud using Strömgren photometry; this technique can be used to derive the absolute magnitude and reddening of most classes of main sequence stars (Strömgren 1966). High accuracy is achievable provided a large number of pertinent standards are observed. Thirty-six of 100 stars we studied met all criteria required for the determination of both distance and color excess; the majority of the stars rejected were metal-poor reddened giants and stars that had evolved somewhat off the main sequence. Fifteen of the acceptable stars were at distances greater than 200 pc and provide no information of relevance to the cloud distance. The color excess vs. distance for the remaining 21 stars in the 16 square degrees centered on

the cloud show the presence of a cloud in the direction of the EUV shadow that is at a distance of $\leq$40 pc.

We derived the emission measure for the plasma in the line of sight to the cloud by folding the *EUVE* deep survey count rate in the direction of the cloud, 0.437 ± 0.02 counts s^{-1}, with the Landini & Fossi code for a temperature of 7×10^5 K. The emission measure in the direction of the cloud is found to be 0.0077 cm^{-6} pc.

Combining the results in Equation 1.1, we immediately obtain the pressure of the hot phase of the ISM in the direction of the absorbing feature. Using a distance to the cloud of 40 pc, we find the pressure is $p/k = 19000$ K cm^{-3}. Because we do not have unreddened stars in the direction of the cloud at distances less than 40 pc, the cloud could, in principle, be closer. In that case the pressure would be even higher.

The McKee-Ostriker model (1977) assumes eventual pressure equilibrium between cool denser clouds and the hot phase of the ISM. The pressure at any particular location is established by the effects of past supernovas. The pressure of the local cloud surrounding the Sun has been well established by a variety of techniques, the most direct is through the analysis of solar HeI 584 Å radiation resonantly scattered by helium in the inflowing cloud. The pressure obtained for the local cloud is 730 ± 30 cm^{-3}K. (Frisch 1994)

There has been a general belief that the pressure of the local bubble is larger than the local cloud, but because of the penetrating power of X-rays it is not clear where this higher temperature/pressure gas originates. This radiation may be produced nearby, or further away, or from a boundary wall, or from all these locations. Wherever its origin, the flux would be modified by absorption by unknown amounts of intervening cooler material.

However, we can now, for the first time, compare two direct measurements of the pressure of nearby ISM material that has experienced the same supernovae shock conditions: (1) the pressure of the parcel of gas in the path between the Sun and the cloud reported here, and (2) the pressure of the local interstellar cloud flowing through the solar system. It is almost superfluous to note that the shock conditions are the same for these two local components. There has been no recent supernovae in this region and Frisch (1994) and Bertin et al. (1993) have provided independent evidence that this region has not been violently heated within the past million years. Hence material in this region has had more than sufficient time to establish pressure equilibrium as per the McKee-Ostriker hypothesis.

The wide difference between the pressure of the local solar cloud and the pressure of the hot quiescent EUV emitting material discussed here directly challenges the underlying concepts of the McKee-Ostriker model.

2. The Ionization State of the ISM

The ionization state of the ISM depends on only a few key mechanisms which produce this ionization, hence a measurement of this parameter will provide crucial information on the current status and evolution of the ISM. This topic has been the subject of over a dozen studies; the results before EUV observations were essentially a scatter plot in a χ_H, χ_{He} diagram.

Hot white dwarfs ($T_{\rm eff} \geq 25,000$ K) are copious sources of EUV continuum radiation, making them excellent objects to use in studying the ISM. Interstellar column densities of hydrogen and both neutral and singly ionized helium can be directly obtained from their EUV absorption signature in hot white dwarf spectra given the known wavelength dependence of the photoelectric absorption and the photoionization edges of He I at 504

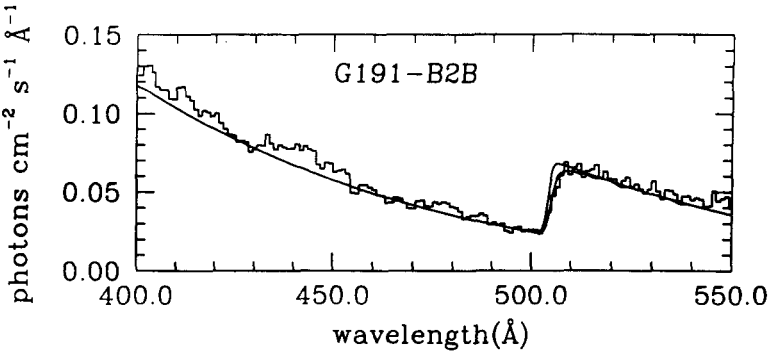

FIGURE 1. Absorption edge of the He I seen in the spectrum of the hot white dwarf G191-B2B.

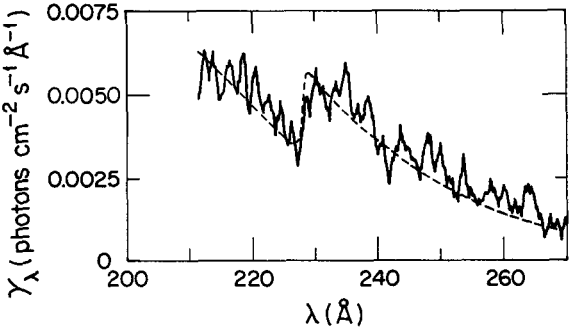

FIGURE 2. Absorption edge of He II seen in the spectrum of the hot white dwarf GD 246.

Å and of He II at 228 Å. This technique offers a direct and model independent way of measuring densities for the main constituents of the ISM.

A measurement of the He I/H I made at longer EUV wavelengths from a sounding rocket observation of the hot white dwarf G191-B2B (Green et al. 1990) resulted in a ratio greater than 10 suggesting that hydrogen is not preferentially ionized in the ISM. Further observations at longer EUV wavelengths by the Hopkins Ultraviolet Telescope of the hot white dwarfs G191-B2B and HZ 43 (Kimble et al. 1993a; 1993b) led to similar conclusions but also opened the prospect of preferential ionization of helium.

The comprehensive wavelength coverage of the *EUVE* spectrographs offers the capability of direct, model independent measurements of both neutral and ionized helium in the ISM. In Figure 1 I show an example of absorption due to interstellar He I. In Figure 2 I show an example of absorption due to interstellar He II. The power of these observations for ISM studies is immediately obvious. *EUVE* has observed several white dwarfs for which a determination of the interstellar column densities of H I, He I, and He II is possible. Vennes et al. (1993) and Dupuis et al. (1995) have used these spectra to explore this topic. In Table 3 I show the result of these analyses and Figure 3 summarizes the most important features. The Vennes et al. (1993) result provides direct spectral data of the He II edge in the hot white dwarf GD 246 that shows helium is ionized at 25% in this view direction, while hydrogen is certainly less than 25% ionized and may be much less; and the work by Dupuis et al. (1995) shows, using similar data on the He I edge, that H I/He I = 14 and that the hydrogen is predominantly neutral.

https://doi.org/10.1017/S025292110003606X Published online by Cambridge University Press

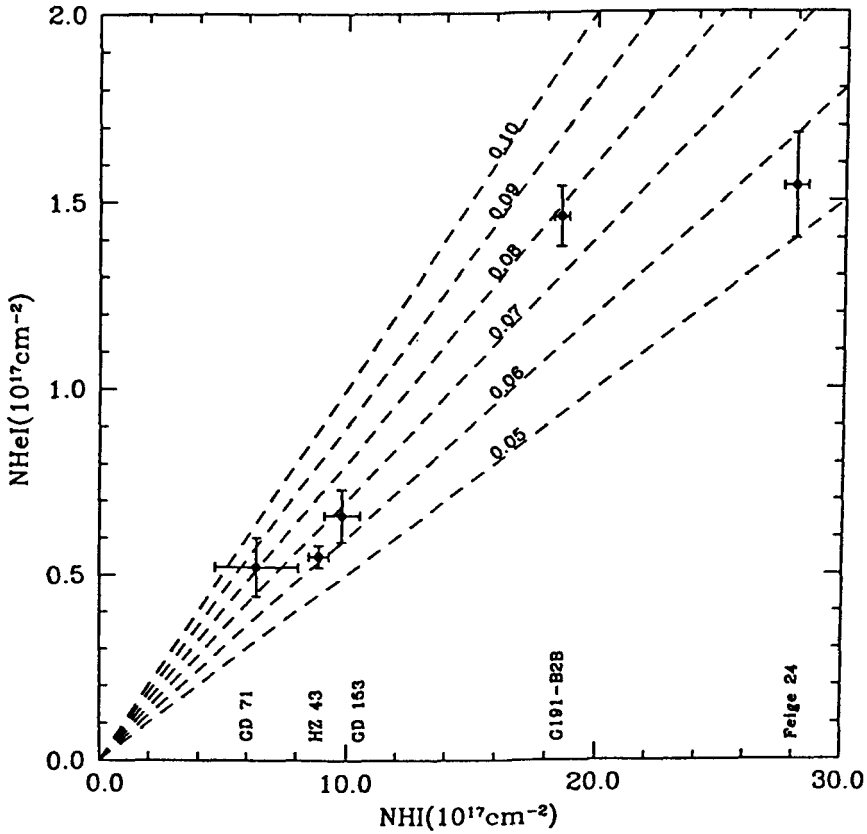

FIGURE 3. The neutral helium and hydrogen columns toward a number of hot white dwarfs.

This work was supported by NASA contract NAS5-30180.

REFERENCES

BERTIN, P., LALLEMENT, R., FERLET, R., & VIDAL-MADJAR, A. 1993, A&A, 278, 549
BOWYER, S., LIEU, R., SIDHER, S. D., LAMPTON, M., & KNUDE, J. 1995, Nature, 375, 212
BURROWS, D. N., & MENDENHALL, J. A. 1991, Nature, 351, 629
COX, D. P., & REYNOLDS, R. J. 1987, ARA&A, 25, 303
DUPUIS, J., ET AL. 1995, ApJ, submitted
FRISCH, P. C., & YORK, D. G. 1983, ApJ, 272, L59
FRISCH, P. C. 1994, Science, 265, 1423
GREEN, J., JELINSKY, P., & BOWYER, S. 1990, ApJ, 359, 499
JAKOBSEN, P., & KAHN, S. M. 1986, ApJ, 309, 682
JENKINS, E. B., JURA, M., & LOEWENSTEIN, M. 1983, ApJ, 270, 88
KIMBLE, R. A., ET AL. 1993a, ApJ, 404, 663
KIMBLE, R. A., DAVIDSEN, A. F., LONG, K. S., & FELDMAN, P. D. 1993b, ApJ, 408, L41
LIEU, R., SUMNER, T. J., BOWYER, S., & SIDHER, S. D. 1993, BAAS, 25 #2, 860
MARTIN, C. & BOWYER, S. 1990, ApJ, 350, 242

MCKEE, C., & OSTRIKER, J. 1977, ApJ, 218, 148

PARESCE, F. 1984, AJ, 89, 1022

SHULL, J. M., & SLAVIN, J. D. 1994, ApJ, 427, 784

SPITZER, L., JR. 1990, ARA&A, 28, 71

SNOWDEN, S. L., MEBOLD, U., HIRTH, W., HERBSTMEIER, U., & SCHMITT, J. H. M. M. 1991, Science, 252, 1529

SNOWDEN, S. L., MCCAMMON, D., & VERTER, F. 1993, ApJ, 409, L21

STRÖMGREN, B. 1966, ARA&A, 4, 433

VENNES, S., DUPUIS, J., RUMPH, T., DRAKE, J., BOWYER, S., CHAYER, P., & FONTAINE, G. 1993, ApJ, 410, L119